*Korean J. Chem. Eng.*, 40(12), 2975-2981 (2023)
DOI: 10.1007/s11814-023-1544-6

pISSN: 0256-1115
eISSN: 1975-7220

# Conductivity enhancement in $K^+$-ion conducting solid polymer electrolyte [PEG : $KNO_3$] and its application as an electrochemical cell

**Anji Reddy Polu*,†, Aseel Abdulameer Kareem**, Kwangmin Kim***, Dongkyu Kim****, Mekala Venkanna*, Hussein Kh. Rasheed**, and Kanapuram Uday Kumar*****

*Department of Physics, BVRIT HYDERABAD College of Engineering for Women, Hyderabad-500090, Telangana, India
**Department of Physics, College of Science, University of Baghdad, Baghdad, Iraq
***Hyundai Corporation, Seoul 03143, Korea
****Advanced Functional Polymers Centre, Korea Research Institute of Chemical Technology (KRICT), Daejeon 34114, Korea
*****Department of Physics, NIT Warangal, Warangal-506004, Telangana, India
(*Received 21 June 2023 • Revised 21 July 2023 • Accepted 6 August 2023*)

**Abstract**−The solution-cast method was used to prepare new solid polymer electrolytes (SPEs) that conduct potassium ions and are based on polyethylene glycol (PEG) complexed with potassium nitrate ($KNO_3$). This polymer electrolyte system was characterized using different experimental techniques, such as X-ray diffraction (XRD), differential scanning calorimetry (DSC), composition vs. conductivity, temperature vs. conductivity, frequency-dependent conductivity, and dielectric measurements. The degree of crystallinity decreased with increasing salt concentration, according to the X-ray diffraction and DSC patterns of PEG with $KNO_3$ salt. For PEG : $KNO_3$ (80 : 20) composition, an optimum conductivity of $8.24\times10^{-6}$ S/cm was recorded at 30 °C. Compared with pure PEG, the optimum conducting composition (OCC) conductivity increased by two orders of magnitude. The temperature range of 303 to 333 K was used for the temperature-dependent conductivity experiments. The findings demonstrate that the conductivity obeys the Arrhenius rule and increases as the temperature rises. A dc plateau and a dispersive zone were observed in the conductance spectrum, which also follows Jonscher's power law. It was investigated how temperature and frequency affect the dielectric permittivity. An electrochemical cell with the configuration K/(80PEG : 20$KNO_3$)/($I_2$+C+electrolyte) was constructed using an 80 : 20 electrolyte system, and its discharge properties were investigated. The cell's open circuit voltage was measured at 2.48 V.

Keywords: PEG, Polymer Electrolyte, Conductivity, Dielectric Constant, Electrochemical Cell

## INTRODUCTION

Researchers over the past 40 years have improved polymer electrolytes for use in viable rechargeable batteries, fuel cells, supercapacitors, and solar cells [1-4]. Solid electrolytes have many benefits over liquid electrolytes, including not leaking, being lightweight, having flexible geometry, being easy to produce, not internally shorting, and being able to reduce battery size [5-7]. In 1979, the first solid polymer electrolyte-based battery was practically proved after the first ion-conducting solid polymer electrolyte was disclosed in 1973 [8,9]. Since then, several types of mobile ionic species, including charge carriers like $Ag^+$, $Li^+$, $Na^+$, $K^+$, $Mg^{2+}$, $Zn^{2+}$, and $Cu^{2+}$, have been observed in solid-state ionic materials [10-16]. The ionic conductivity increased as the salt concentration increased; however, the weak mechanical strength and potential stability of these polymer electrolytes are their main. drawbacks Gao et al. explained that single-ion conducting polymer electrolytes are key materials for next-generation battery applications [17]. The lithium salts LiTDI and LiDFOB were successfully tested in PEO matrix systems, proving to be a promising, improved electrolyte for lithium-ion batteries [1,18]. After incorporating InAs nanowire fillers, PEO/PVP doped with sodium hexafluorophosphate solid polymer electrolytes showed high sodium ionic conductivity, which is approximately $1.50\times10^{-4}$ $Scm^{-1}$ at 40 °C. This is one of the better electrolyte materials for the next generation of high-capacity, high-performance, and inexpensive batteries [19].

Li and Na have smaller ionic radii than potassium (K), which is 1.33 Å. Because of the greater radius, the potassium salts' activation energy is lower. K salt has a higher level of salt salvation because of its lower lattice energy. Potassium metal can be employed in a wider variety of technologies due to its softness. Compared to lithium, potassium is far more plentiful, cheaper, and less moisture-resistant [20]. A key activity in this scenario is the synthesis of polymer electrolytes either from sustainable resources or waste-derived products. Potassium batteries have intriguing features as large-scale energy storage systems [21]. In the field of large-scale energy storage, sodium-ion batteries (SIBs) and potassium-ion batteries (KIBs) are viewed as viable alternatives to lithium-ion batteries (LIBs) due to the low cost of sodium/potassium resources and similar electrochemical characteristics of $Na^+/K^+$ to $Li^+$ [16].

Potassium salts, which differ from Li-ion conducting electrolytes in that they are made up of molecularly flexible anions with a substantially delocalized electron density, can be used to create K-ion conducting gel polymer electrolytes and solid-state polymer elec-

†To whom correspondence should be addressed.
E-mail: reddyphysics06@gmail.com

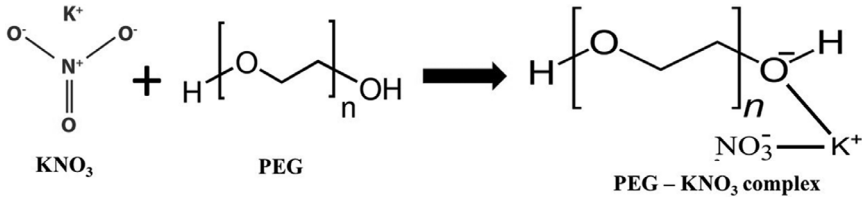


**Fig. 1. Interaction scheme between PEG and $KNO_3$.**

trolytes. Recently, a water-free potassium ion-conducting polymer electrolyte was successfully synthesized and used in an all-solid-state half-cell with a fluorine-containing salt, the potassium bis(fluorosulfonyl)imide (KFSI) [22]. PEO-KFSI electrolyte films demonstrated high conductivity values up to $10^{-4}$ S/cm at 60 °C. On the other hand, a conductivity value of $1.36\times10^{-5}$ S $cm^{-1}$ was reported at room temperature for poly(propylene carbonate)-KFSI polymer electrolytes, despite the fact that flammable liquid electrolytes are inherently riskier than these solid-state electrolytes [23,24].

Large molecular weight polymers ($10^6$) like poly (ethylene oxide) (PEO) are the most fully explored among the documented polymer systems in terms of polymer complexation behavior with various metal salts [25,26]. Ionic conductivity and electrochemical cell performance of PEO-$KNO_3$ solid polymer electrolytes have been examined by Sreekanth and Rao [27]. Low molecular weight polymers like PEG, however, have received relatively few publications [28,29]. PEO and PEG have comparable structures and share repeating units; it is anticipated that the metal salt complexes of the PEG system will have high ionic conductivity comparable to that observed in the PEO systems.

Keeping these facts in mind, we synthesized the solid polymer electrolytes by mixing $KNO_3$ salt with PEG in the current study. Our findings show that the ionic conductivity of the solid polymer electrolytes increases when $KNO_3$ is added to the PEG matrix. XRD and DSC measurements were used to characterize the resulting electrolyte films. Using the ac impedance analysis technique, the conductivity of the solid polymer electrolytes was determined in the temperature range of 303-333 K.

**1. Role of $KNO_3$ as Dopant**

The chemical formula of potassium nitrate is $KNO_3$. It is a salt made up of potassium ions ($K^+$) and nitrate ($NO_3$) ions. It is a naturally occurring solid source of nitrogen that appears as a mineral niter. One of the nitrogen-containing substances referred known as saltpeter is potassium nitrate [30]. At room temperature, the substance has an orthorhombic crystal structure and is soluble in water. $KNO_3$ was chosen because it mixes up quite well in the solution. When introduced into polymers, this ionic salt is extremely important for the enhancement of the structural, thermal, and electrical properties of ion transport systems. This is a helpful criterion to employ when designing a battery electrolyte medium with proper composition and performance goals in mind. The exact ionic bonding scheme of PEG moiety with $KNO_3$ is represented as follows (Fig. 1).

## EXPERIMENTAL

**1. Materials**

Polyethylene glycol (PEG) from CDH, India, with a molecular weight of 4,000 was dried at 35 °C under vacuum for 48 h. $KNO_3$ (98%, CDH, India) was vacuum-dried for 24 hours at 35 °C. We used solvent as distilled water to prepare the PEG-inducted $KNO_3$ solution.

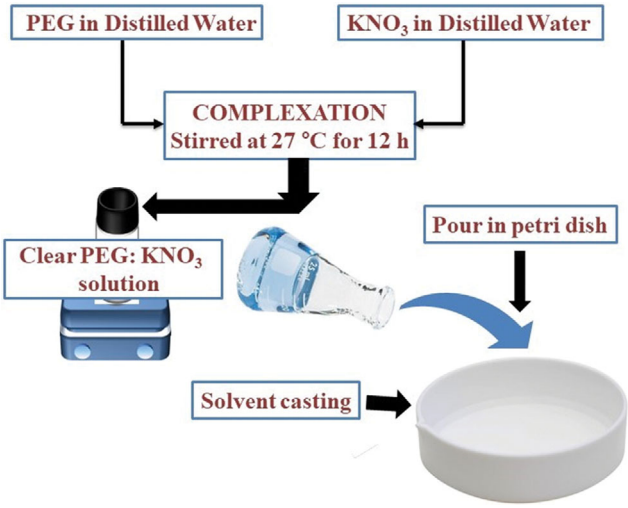


**Fig. 2. Synthesis process of solid polymer electrolytes.**

**2. Solid Polymer Electrolyte Preparation**

The solid polymer electrolyte films of pure PEG and PEG combined with $KNO_3$ were prepared by using solution blending and controlled weight loading ratios of 100 : 0, 90 : 10, 85 : 15, 80 : 20, and 70 : 30. The system's homogeneity was attained after 12 hours of steady stirring at room temperature. The solution was then poured into glass Petri dishes where it slowly evaporated in a vacuum at ambient temperature. In a controlled situation, the solvent evaporated and the films peeled off. After that, the polymer electrolyte samples were put into desiccators to dry out even more before the test. Fig. 2 depicts the synthesis of solid polymer electrolytes.

**3. Characterization**

The nature of the synthesized polymer electrolyte systems was investigated using WAXD Philips X'Pert PRO diffractometer (Almelo, the Netherlands), using a graphite monochromator on the diffracted beam and operating in the reflection geometry (CuK$\alpha$ radiation). The thermal response was studied by differential scanning calorimetry (TA Instruments model 2920 calorimeter) in a static nitrogen atmosphere at a heating rate of 5 °C per minute in a temperature range of 0 to 100 °C. Using a HIOKI 3532-50 LCR Hitester, impedance measurements were made in the temperature range of 303-333 K over the frequency range of 100 Hz to 1 MHz. The following formula was used to determine the ionic conductivity from the measured bulk resistance, thickness, and area of the polymer film:

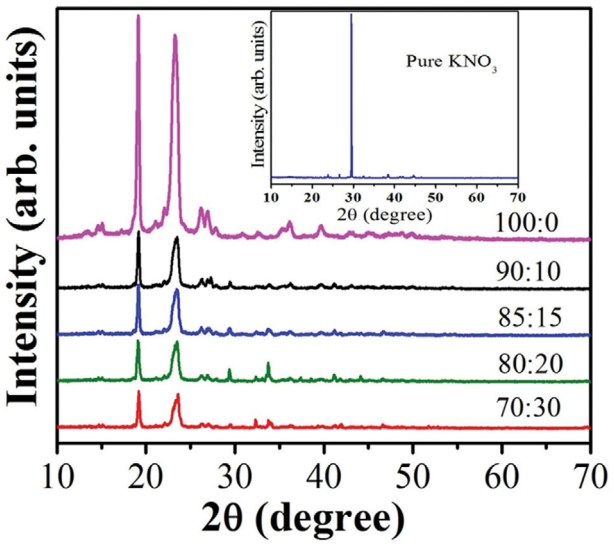


**Fig. 3. XRD patterns of pure PEG, pure $KNO_3$, and PEG complexed with $KNO_3$ polymer electrolyte films.**

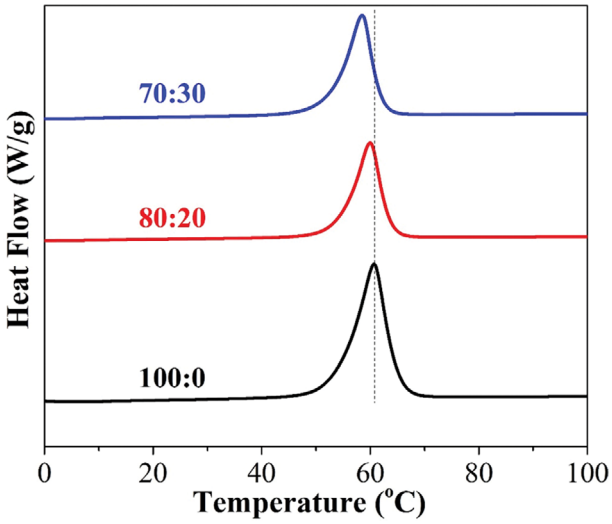


**Fig. 4. DSC traces of different concentrations of PEG : $KNO_3$ polymer electrolytes.**

$$\sigma = \frac{t}{R_b A}$$

where t is the polymer electrolyte's thickness (measured in cm) using a micrometer screw gauge, A is the blocking electrode contact's area (measured in $cm^2$), and $R_b$ is the bulk resistance (measured in Ω). Electrochemical solid-state cells with the configuration K/(80PEG : 20$KNO_3$)/($I_2$+C+electrolyte) were prepared under a constant load of 100 kΩ.

## RESULTS AND DISCUSSION

### 1. X-ray Diffraction Studies

In order to evaluate the structure of the polymer electrolyte samples and look into the occurrence of complexation, X-ray diffraction experiments were conducted. Fig. 3 displays the XRD patterns of the pure PEG, pure $KNO_3$, and polymer complexes of PEG : $KNO_3$ (90 : 10, 85 : 15, 80 : 20, and 70 : 30). Although the mechanism of ionic transport in polymer electrolytes is currently poorly understood, polymer chains that are present in the amorphous phase or domain are significantly in motion while not conducting in the crystalline phase. The diffraction peaks between $2\theta$=19.2° and 23.4° in the PEG : $KNO_3$ solid polymer electrolyte films are less intense when compared to the X-ray diffraction patterns of pure PEG and pure $KNO_3$. This shows that when salt concentration increases, PEG's degree of crystallinity decreases. In the polymer complexes, the major peak at $2\theta$=29.1° that is found in pure $KNO_3$ is still there but is less intense. The creation of polymer-salt complexation is confirmed by the results above. The degree of crystallinity and peak intensity is correlated, according to Hodge et al. [31]. Amorphous polymers with flexible backbones can achieve this amorphous character, which leads to increased high ionic conductivity and ionic diffusivity [32].

### 2. DSC Analysis

The thermal behavior of the PEG : $KNO_3$ polymer complex systems was investigated using DSC. Fig. 4 displays the DSC traces of pure PEG and PEG : $KNO_3$ polymer electrolyte complexes with 20 wt% and 30 wt% of $KNO_3$. Table 1 provides a summary of the DSC results. These PEG : $KNO_3$ SPEs exhibit a distinct endothermic peak at a temperature of about 60 °C, which is consistent with the typical melting of crystalline PEG. It is important to note that the melting point ($T_m$) of these SPEs rises with decreasing K salt concentration in the PEG : $KNO_3$ (100 : 0, 80 : 20, and 70 : 30) blended electrolytes (Table 1). This could be attributed to the plasticizing effects of K salt on these SPEs. The DSC traces show a pattern that is consistent with the earlier findings [13,14]. The relative percentage of crystallinity ($X_c$) was computed using the following equation under the assumption that pure PEG was 100% crystalline.

**Table 1. DSC results of PEG : $KNO_3$ polymer electrolytes**

| Electrolyte sample PEG : $KNO_3$ | Melting point ($T_m$) (in °C) | $H_m$ (J/g) | $X_c$ (in %) |
|---|---|---|---|
| 100 : 0 | 60.62 | 204.3 | 100 |
| 80 : 20 | 59.68 | 134.6 | 65.88 |
| 70 : 30 | 58.56 | 145.4 | 71.16 |

$$X_c = \left(\frac{\Delta H_m}{\Delta H_m^0}\right) \times 100\%$$

where $\Delta H_m^0$ is the standard enthalpy of fusion of pure PEG (i.e., 204.3 J/g) and $\Delta H_m$ is the enthalpy of fusion of the SPEs. A decrease in the degree of crystallinity and the predominance of amorphous phase, which is also verified by the XRD results, are clearly indicated by a decreasing of the $T_m$ and broadening of the melting endotherm.

### 3. Composition Dependent Conductivity Studies

Complex impedance spectroscopy was employed to assess the conductivity of the PEG with $KNO_3$ electrolytes. In complex impedance graphs, the intersection of the high-frequency and real axes yields the bulk resistance ($R_b$). Fig. 5 shows the variation in conductivity ($\sigma$) as a function of the salt concentration of $KNO_3$ in

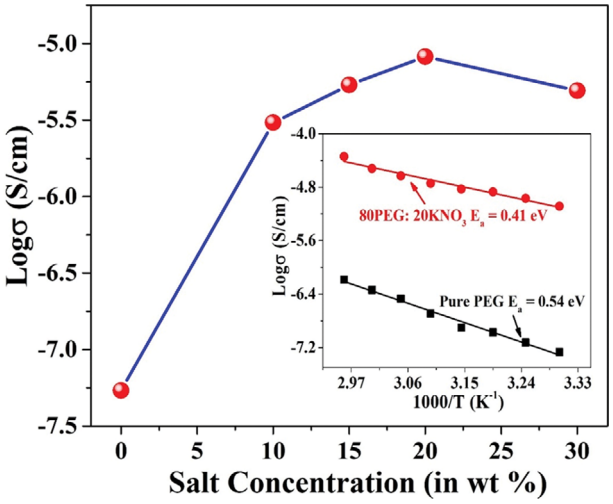


**Fig. 5. Ionic conductivity versus $KNO_3$ concentration at 303 K. Temperature-dependent conductivity is in the inset**

PEG at 303 K. According to the findings, pure PEG conductivity is approximately $5.41\times10^{-8}$ S/cm at 303 K, but it rises rapidly to $8.24\times10^{-6}$ S/cm in PEG with 20 weight percent $KNO_3$ salt. When compared to pure PEG polymer film, the conductivity of these polymer electrolyte films is observed to increase by more than two orders. The change from a semi-crystalline phase to an amorphous phase of the polymer complexes caused by the dispersion of $KNO_3$ can be attributed to physical interactions between the polymeric chain and salt, which can also be used to explain why the generated polymer electrolytes have improved ionic conductivity. Up to a certain salt concentration, increased $KNO_3$ salt allows the segmental mobility of the polymeric chain to increase. After that point, however, rising salt concentrations lead the ion pairs to group together into ionic clusters, further reducing ionic mobility. These ionic clusters are less mobile, which can promote the formation of crosslinks and stiffen the polymeric matrix. A considerable drop in ionic conductivity was seen at greater concentrations, and it has been reported that ionic conductivity increases with an increase in salt content by up to 20 wt%.

The number of mobile charge carriers and the amorphousness of the polymer electrolyte increased along with the salt concentration, which caused the conductivity to increase. On the other hand, for the mixture containing 30 wt% of salt, a decrease in conductivity was seen. This was brought on by ion aggregation, which reduced the number of mobile charge carriers present per unit volume and decreased ion mobility [33].

Furthermore, a reduction in free volume in the polymer matrix brought on by the buildup of $KNO_3$ salt might cause conformational changes in the polymer chains, which can prevent ions from being inserted into or ejected from the polymer electrolyte surface [34]. Therefore, once the salt content exceeded 20 wt%, a correlation between a drop in free volume and a decrease in ionic conductivity can be found.

## 4. Temperature-dependent Conductivity Studies

Studies on the relationship between conductivity and temperature were performed on PEG : $KNO_3$ SPEs with 0 wt% and 20 wt% $KNO_3$ salt. The films were tested for a.c. impedance in the 303 K to 333 K temperature range while sandwiched between two blocking electrodes. According to Fig. 5 (inset), which is largely linear with activation energy, $E_a$ for the films containing 0 wt% and 20 wt% of $KNO_3$ falls between 0.54 and 0.41 eV. The plot of logσ vs 1000/T's regression value, $R^2$, is nearly one, indicating that the plot can be regarded as linear and that it follows the Arrhenius behavior. With the insertion of 20 weight percent of $KNO_3$ into PEG, the activation energy is reduced. This shows that the addition of salt increases the amorphous nature of the polymer electrolyte membrane, which facilitates ionic transport mobility in the polymer network. The polymeric chain's increased flexibility allows it to improve the segmental motion of the host polymer [35].

The free volume model can be used to show how conductivity increases with temperature. As the temperature rises, the polymer can easily expand and create free volume. As a result, the free volume increases along with the temperature. The free volume surrounding the polymer chains determines the final conductivity, which is represented by the overall mobility of ions and the polymer. Ions, solvated molecules, or polymer segments may therefore travel into the free volume when the temperature rises. This causes a rise in ion mobility and segmental mobility, which facilitates ion transport and successfully offsets the obstructive impact of the ion cloud [36].

## 5. Frequency-dependent Conductivity Studies

Figs. 6 and 7 illustrate the logarithmic conductivity as a function of logarithmic frequency for PEG : $KNO_3$ polymer electrolytes with various compositions at 303 K and that for the 80PEG : 20$KNO_3$ polymer complex at various temperatures, respectively. The frequency-dependent conductivity plots display two separate zones, as seen in the pictures. The frequency-independent conductivity correlates with the first region seen at low frequencies. The bulk conductivity of the sample was given this conductivity value ($\sigma_{dc}$). The conductivity rises with frequency in the high-frequency domain. Extending the plateau region to the Y-axis was used to determine the $\sigma_{dc}$ value. The highest conductivity for the 80PEG : 20 $KNO_3$

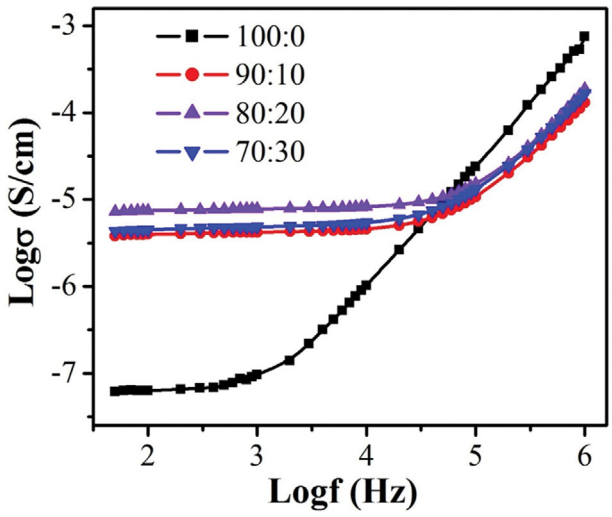


**Fig. 6. Conductance spectra of PEG : $KNO_3$ with different salt concentrations at 303 K.**

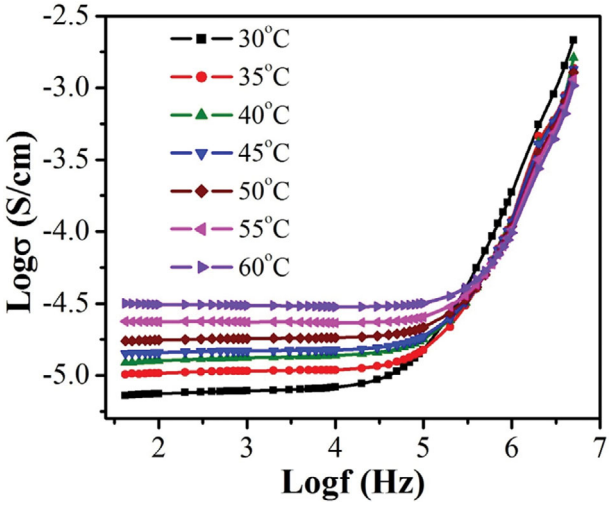


**Fig. 7. Conductance spectra of 80PEG : 20$KNO_3$ polymer electrolyte at different temperatures.**

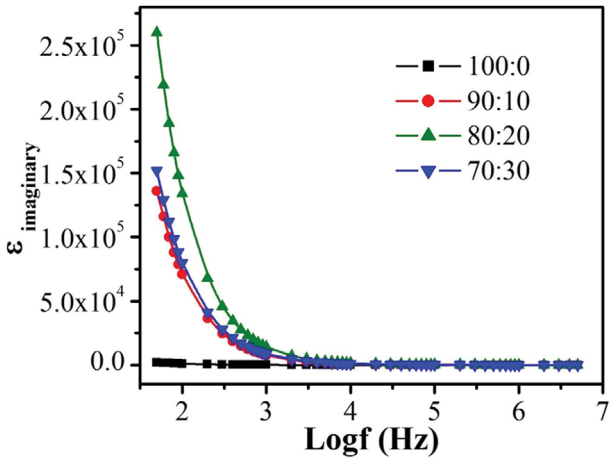


**Fig. 8. Variation of $\varepsilon_{imaginary}$ vs. logf at 303 K.**

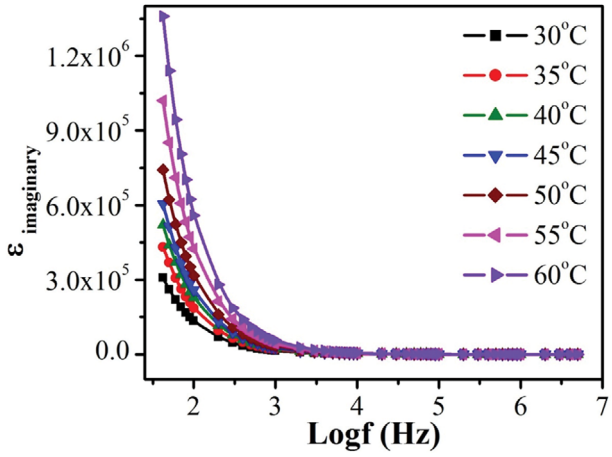


**Fig. 9. Typical plots of variation of the imaginary part of dielectric constant with frequency for sample 20 wt% of salt at different temperatures.**

polymer electrolyte was determined to be $7.92\times10^{-6}$ S/cm at 303 K.

It has been discovered that the values for bulk conductivity derived from the impedance plot agreed with the dc conductivity values acquired from conductance spectra. According to Fig. 7, the dc conductivity rises as the temperature rises, which shows that the free volume surrounding the polymer chain is what enhances the conductivity as a result of the mobility of ions and polymer segments.

It is generally accepted that as the degree of crystallinity reduces or, to put it another way, as the polymeric backbone's pliability increases, the conductivity rises. The amorphous region is growing because of an increase in free volume, whereas the crystalline portions restrict ion mobility by restricting the ions' routes. The increase in free volume makes it easier for ions to move across the amorphous area by facilitating the passage of ionic charges [37]. A reduction in the degree of crystallinity and the predominance of the amorphous region are linked to the increase in conductivity in this PEG system with an increase in salt.

**6. Dielectric Analysis**

The dielectric spectroscopic analysis of the PEG : $KNO_3$ polymer electrolytes was examined in light of the electrolytes' dielectric permittivity. In essence, the dielectric experiments revealed that the transport mechanism of $KNO_3$ salt ions across the PEG polymer chain electrolytes was mostly caused by the hopping mechanism coupled with the segmental motion of the polymer chain [38]. The material's dielectric constant illustrates the polarization of the material during the formation of the hetero-charge layer, which is brought on by finite and reversible trapped ions deposited at the electrode-electrolyte interface [39].

Fig. 8 shows the frequency dependence of the imaginary component of the dielectric constant curve for all samples at room temperature (303 K). As frequency rises, the imaginary portion of the dielectric constant falls until it reaches saturation at higher frequencies. The buildup of charge carriers close to the electrodes is the likely cause of the high dielectric constant at low frequencies. The increased charge carrier density at the space charge accumulation zone, which led to an increase in the equivalent capacitance, is what causes the higher values of the dielectric constant for 20 weight percent of $KNO_3$ (greater conductivity). The high periodic reversal of the applied field causes the dielectric constant to decrease at higher frequencies [40].

The dielectric constant, $\varepsilon_{imaginary}$, against logf of 80PEG : 20$KNO_3$ at different temperatures is shown in Fig. 9. The charts make it obvious that the values of $\varepsilon_{imaginary}$ decline with frequency and stabilize at higher frequencies. At low frequencies, the values of $\varepsilon_{imaginary}$ are high, but as the frequency of the field increases, the values start to fall. This could be because the dipoles can no longer follow the field variation at higher frequencies as well as because of the polarization effects. It has been determined that the charge build-up at the electrode-electrolyte interface is what causes the low-frequency dispersion area. The periodic reversal of the electric field happens so quickly at higher frequencies that there is not any extra ion diffusion in the field's direction.

Polar and non-polar polymers exhibit variations in dielectric permittivity as a function of temperature. The dielectric permittiv-

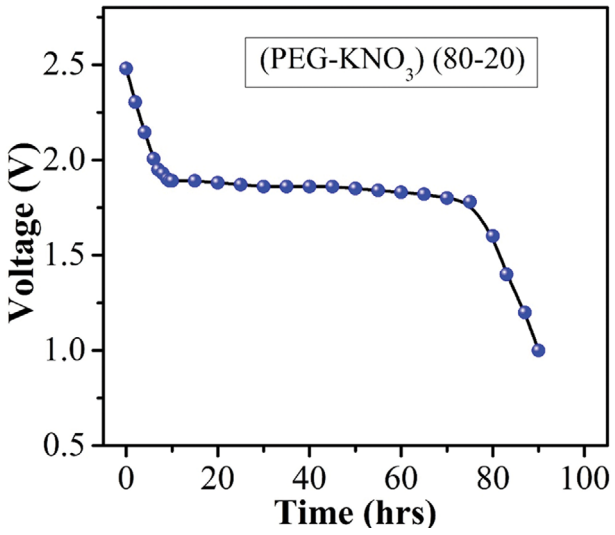


**Fig. 10. Discharge characteristic plot of PEG : $KNO_3$ (80 : 20) electrochemical cell for a constant load of 100 kΩ.**

**Table 2. Cell parameters of (80PEG : $20KNO_3$) electrolyte cell for a constant load of 100 kΩ**

| Cell parameters | K/[80PEG : $20KNO_3$]/ ($I_2$+C+electrolyte) |
|---|---|
| Open circuit voltage (OCV) | 2.48 V |
| Cell weight | 1.58 g |
| Area of the cell | 1.33 $cm^2$ |
| Short circuit current (SCC) | 324 μA |
| Load | 100 kΩ |
| Time for plateau region | 65 h |
| Specific power density | 21.54 mW/kg |
| Specific energy density | 1,355.31 mWh/kg |

ity of polar polymers often rises with temperature. The dielectric permittivity of non-polar polymers, however, is temperature-independent [41]. This behavior is characteristic of polar dielectrics, in which the permittivity increases as temperature rises by facilitating the orientation of dipoles.

**7. Electrochemical Cell Discharge Characteristics**

In Fig. 10, the discharge profiles of the configuration of solid-state electrochemical cells K/(80PEG : $20KNO_3$)/($I_2$+C+electrolyte) are depicted. The voltage dropped quickly at first, which may have been caused by polarization or the emergence of a potassium salt thin layer at the electrode-electrolyte interaction [42]. Table 2 contains open circuit voltage (OCV), short circuit current (SCC), and other cell characteristics of the cell. The SCC and the discharge duration for the plateau region are found to match with earlier findings published by other researchers [27,43]. This system's strong ionic conductivity and increased amorphousness, as shown in the 80PEG : $20KNO_3$ polymer electrolyte system, have been explained.

## CONCLUSION

By using the solution casting approach and distilled water as the solvent, PEG with $KNO_3$-based polymer electrolytes of various weight percentages were prepared. The XRD and DSC analysis shows that salt and polymers can create complex structures and that the polymer complex is amorphous. At room temperature, an 80PEG : $20KNO_3$ film was shown to have a maximum conductivity of $8.24\times10^{-6}$ S/cm. Arrhenius behavior was observed in pure PEG and 80PEG : $20KNO_3$ samples. From the analysis of the Arrhenius plot, it has been determined that the activation energy falls with the addition of $KNO_3$ salt for both samples of pure PEG and 80PEG : $20KNO_3$. The characteristics of an electrochemical cell were established using the solid polymer electrolyte 80PEG : $20KNO_3$. With these specifications, the manufactured polymer electrolyte is guaranteed to be a strong contender for low-cost polymer electrolyte membranes for solid-state batteries.

## REFERENCES

1. A. R. Polu, A. A. Kareem and H. K. Rasheed, *J. Solid State Electr.*, **27**, 409 (2023).
2. S. H. Woo, S. Kim, S. Woo, S. H. Park, Y. S. Kang, N. Jung and S. D. Yim, *Korean J. Chem. Eng.*, (2023) https://doi.org/10.1007/s11814-023-1474-3.
3. M. Hwang, J. S. Jeong, J. C. Lee, S. Yu, H. S. Jung, B. S. Cho and K. Y. Kim, *Korean J. Chem. Eng.*, **38**, 454 (2021).
4. R. Singh, A. R. Polu, B. Bhattacharya, H. W. Rhee, C. Varlikli and P. K. Singh, *Renew. Sust. Energ. Rev.*, **65**, 1098 (2016).
5. A. R. Polu, P. K. Singh, P. Siva Kumar, G. M. Joshi, T. Ramesh, I. M. Noor, A. Y. Madkhil and S. Kakroo, *High Perform. Polym.*, **35**, 4 (2023).
6. B. H. Lim, J. M. Kim, V. T. Nguyen, H. Kim, C. W. Park, J. K. Lee, C. H. Lee, J. Yoo, B. K. Min and S. K. Kim, *Mater. Today, Energy*, **33**, 101263 (2023).
7. J. P. Hoffknecht, A. Wettstein, J. Atik, C. Krause, J. Thienenkamp, G. Brunklaus, M. Winter, D. Diddens, A. Heuer and E. Paillard, *Adv. Energy Mater.*, **13**, 2202789 (2023).
8. D. E. Fenton, J. M. Parker and P. V. Wright, *Polymer*, **14**, 589 (1973).
9. M. P. Armand, J. M. Chabagno and M. Diadat, "Fast Ion Transport in Solids" (Eds.) P. Vashistha, J. M. Mundy and G. K. Sheny, North Holland (1979).
10. Y. An, X. Han, Y. Liu, A. Azhar, J. Na, A. K. Nanjundan, S. Wang, J. Yu and Y. Yamauchi, *Small*, **18**, 2103617 (2022).
11. F. Gebert, J. Knott, R. Gorkin III, S. L. Chou and S. X. Dou, *Energy Stor. Mater.*, **36**, 10 (2021).
12. N. M. Ali, A. A. Kareem and A. R. Polu, *J. Inorg. Organomet. Polym.*, **32**, 4070 (2022).
13. A. R. Polu, R. Kumar and G. M. Joshi, *Ionics*, **20**, 675 (2014).
14. A. R. Polu and R. Kumar, *Bull. Mater. Sci.*, **37**, 309 (2014).
15. S. B. Aziz, R. M. Abdullah, M. F. Z. Kadir and H. M. Ahmed, *Electrochim. Acta*, **296**, 494 (2019).
16. H. Yin, C. J. Han, Q. R. Liu, F. Y. Wu, F. Zhang and Y. B. Tang, *Small*, **17**, 2006627 (2021).
17. J. Gao, C. Wang, D. W. Han and D. M. Shin, *Chem. Sci.*, **12**, 13248 (2021).
18. A. R. Polu, H. W. Rhee, M. J. K. Reddy, A. M. Shanmugharaj, S. H. Ryu and D. K. Kim, *J. Ind. Eng. Chem.*, **45**, 68 (2017).
19. C. Devi, J. Gellanki, H. Pettersson and S. Kumar, *Sci. Rep.*, **11**, 20180

(2021).
20. W. Zhang, Y. Liu and Z. Guo, *Sci. Adv.*, **5**, 7412 (2019).
21. S. Trano, F. Corsini, G. Pascuzzi, E. Giove, L. Fagiolari, J. Amici, C. Francia, S. Turri, S. Bodoardo, G. Griffini and F. Bella, *ChemSusChem*, **15**, e202200294 (2022).
22. Y. Xu, T. Ding, D. Sun, X. Ji and X. Zhou, *Adv. Funct. Mater.*, **33**, 2211290 (2023).
23. M. Elmanzalawy, E. S. Ahijón, O. Kisacik, J. C. González and E. C. Martínez, *ACS Appl. Energy Mater.*, **5**, 9009 (2022).
24. H. Fei, Y. Liu, Y. An, X. Xu, J. Zhang, B. Xi, S. Xiong and J. Feng, *J. Power Sources*, **433**, 226697 (2019).
25. J. Feng, L. Wang, Y. Chen, P. Wang, H. Zhang and X. He, *Nano Convergence*, **8**, 2 (2021).
26. A. R. Polu and H. W. Rhee, *Int. J. Hydrog. Energy*, **42**, 7212 (2017).
27. T. Sreekanth, M. J. Reddy, S. Subramanyam and U. V. Subba Rao, *Mater. Sci. Eng. B*, **64**, 107 (1999).
28. D. Shanmukaraj and R. Murugan, *J. Power Sources*, **149**, 90 (2005).
29. A. R. Polu and R. Kumar, *J. Chem.*, **8**, 628790 (2011).
30. C. S. Joshi, M. R. Shukla, K. Patel, J. S. Joshi and O. Sahu, *Int. Lett. Chem. Phys. Astron.*, **2**, 88 (2015).
31. R. M. Hodge, G. H. Edward and G. P. Simon, *Polymer*, **37**, 1371 (1996).
32. H. M. Alghamdi and A. Rajeh, *Int. J. Energy Res.*, **46**, 20050 (2022).
33. N. M. Ghazali, A. F. Fuzlin, M. A. Saadiah, Md. M. Hasan, Y. Nagao and A. S. Samsudin, *J. Non Cryst. Solids*, **598**, 121939 (2022).
34. J. Zhu, Z. Zhang, S. Zhao, A. S. Westover, I. Belharouak and P. F. Cao, *Adv. Energy Mater.*, **11**, 2003836 (2011).
35. W. H. Meyer, *Adv. Mater.*, **10**, 439 (1998).
36. P. Bashiri, T. Prasada Rao, V. M. Naik, G. A. Nazri and R. Naik, *Solid State Ionics*, **343**, 115089 (2019).
37. M. B. Ahmed, S. B. Aziz and A. R. Murad, *Ionics*, **28**, 5153 (2022).
38. M. Y. Chong, A. Numan, C. W. Liew, K. Ramesh and S. Ramesh, *J. Appl. Polym. Sci.*, **134**, 44636 (2016).
39. F. S. Howell, R. A. Bose, P. B. Macedo and C. T. Moynihan, *J. Phys. Chem.*, **78**, 639 (1974).
40. N. Tripathi, A. Shukla, A. K. Thakur and D. T. Marx, *Electrical conduction in dispersed phase solid polymer electrolytes: The dielectric and electric modulus approach*, (Eds.) J. E. House, In Developments in Physical & Theoretical Chemistry, Dynamic Processes in Solids, Elsevier (2023).
41. M. Irfan, A. Manjunath, S. S. Mahesh, R. Somashekar and T. Demappa, *J. Mater. Sci: Mater. Electron.*, **32**, 5520 (2021).
42. K. Zhang, J. Chen, W. Feng, C. Wang, Y. N. Zhou and Y. Xia, *J. Power Sources*, **553**, 232311 (2023).
43. T. Sreekanth, M. J. Reddy and U. V. Subba Rao, *J. Power Sources*, **93**, 268 (2001).